A journal for the publication of
original research in all branches of physics

www.publish.csiro.au/journals/ajp

Nuclear Orientation on Rare Earth Nickel Alloys*

K. Nishimura

Faculty of Engineering, Toyama University,
Toyama 930, Japan.

Abstract

A hyperfine interaction study of the light rare earth elements, Ce, Pr, Nd and Pm, in the rare earth nickel and $CeNi_2Al_5$ compounds by means of the low temperature nuclear orientation is summarised. The magnitudes and directions of the magnetic hyperfine fields obtained through measurements of γ-ray anisotropy and angular distributions reveal the magnetic structures of the ions. The experiments extracted peculiar results for the magnetic properties of the ions, and show certain novel features of the technique to the study of solid-state magnetism.

1. Introduction

The technique of low temperature nuclear orientation (NO) has been successfully used for the study of hyperfine interactions (Stone and Postma 1986). When the nuclear properties of the probe nuclei are well known, this technique can determine the strengths (B_{HF}) and directions of the hyperfine fields (HF) acting at the nuclei under study. These in turn relate to the magnetisation of the ordered ions and their spatial ordering. Particularly for rare earth ions, in which the main contribution to the HF arises from orbital motion of the localised 4f electrons, magnetic structures can be investigated through such hyperfine interactions.

Since NO is a radioactive detection technique, it can provide some information similar to that from magnetisation measurements and some unique information which is not readily accessible by the conventional techniques used in magnetism. The basis of the NO technique is outlined in the first section of measurements, [142]Pr in PrNi. The sensitivity to distinguish magnetic ions in a material is utilised in the study of Pm ions as an impurity in PrNi and NdNi compounds, using [144]Pm nuclei. The ability to discover non-axial ordering is shown in NO of [141]Ce in a $CeNi_2Al_5$ compound. The identification of the ions responsible for a bulk magnetisation and the direct observation of external field effects upon the ordered system are demonstrated in NO of [147]Nd in the $Ce_xNd_{1-x}Ni$ series and $La_{0.8}Nd_{0.2}Ni$. Finally, a brief comment for future applications is given.

2. Experimental

The present study requires all the samples to be single crystals. We employed two kinds of methods to grow the single crystals: the Czochralski pulling method and Bridgman method after Ar arc-melting. The directions of the crystallographic axes were determined by the X-ray back reflection Laue method. For NO experiments, the crystals were cut into rectangular plates of approximate dimensions $3\times2\times0\cdot1$ mm; the longest side was chosen along the easy magnetisation direction of the compounds.

The samples were irradiated by alpha, deuteron or thermal neutron beams to produce probe radioactive nuclei. The probe nuclei, nuclear reactions and irradiation conditions are as follows:

^{141}Ce : ^{140}Ce(n, γ), thermal neutrons of flux 2×10^{12} cm^{-2} for 7 hours;

^{142}Pr : ^{141}Pr(n, γ), thermal neutrons of flux 2×10^{12} cm^{-2} for 7 hours;

^{144}Pm : ^{141}Pr(α, 2n), 30 MeV α-beam of $0\cdot5$ μA for 30 min;

^{144}Pm : ^{143}Nd(d, n), ^{144}Nd(d, 2n), 25 MeV d-beam of 1 μA for 30 min;

^{147}Nd : ^{146}Nd(n, γ), thermal neutrons of flux 2×10^{12} cm^{-2} for 7 hours.

The resultant radioactivity was several μCi. In the case of ^{144}Pm in NdNi, the estimated concentration of Pm ions is about 1 ppm, which is highest in the present study.

In the simple system, for example a ferromagnetically ordered sample in which all nuclei are oriented with respect to a single hyperfine interaction axis, the observed γ-ray angular distribution (or γ anisotropy) can be interpreted using the expression (Krane 1986):

$$W(\theta) = 1 + f\sum B_\lambda(\mu_{\mathrm{N}},\, B_{\mathrm{HF}},\, T)\, U_\lambda\left(\Delta J_\beta\right) A_\lambda\left(L_\gamma\right) Q_\lambda\, P_\lambda\left(\cos\theta\right),$$

where the factor f denotes the fraction of the nuclei which experience the full B_{HF}, and orientation parameters B_λ describe the degree of orientation, being a summation over the nuclear Zeeman-split substrate Boltzmann distribution (μ_{N} is the nuclear magnetic dipole moment). Nuclear electric quadrupole interactions in the light rare earth ions are typically more than an order of magnitude smaller than magnetic dipole interactions, and are therefore neglected in this work. The $U_\lambda A_\lambda$ parameters depend on the decay scheme of the nuclei under study. The Q_λ are solid angle correction factors for detectors; for the detectors used $Q_2 = 0\cdot98$ and $Q_4 = 0\cdot95$. The Legendre polynomials $P_\lambda(\cos\theta)$ are evaluated at the angle between each detector and the orientation axis. Since γ emission conserves parity, only the even orders of λ arise so that an uniaxial antiferromagnetically ordered system will show the same γ-ray distribution as the ferromagnetic case.

3. Results and Discussion

(3a) NO of ^{142}Pr in PrNi

PrNi was chosen as our first compound to apply this method because the known magnetic structure is simple; PrNi is a ferromagnet with Curie temperature of

20 K, and the magnetically easy direction is the c-axis (Fillion et $al.$ 1984).

A primary purpose of this work was to establish the β-decay mode. The ground state of ^{142}Pr ($I^{\pi} = 2^{-}$) decays via first-forbidden β-decay to the first excited state ($I^{\pi} = 2^{+}$) in ^{142}Nd which de-excites to the 0^{+} ground state, as shown in Fig. 1a (Firestone et $al.$ 1996). For this case, the U_{λ} parameters in the $W(\theta)$ equation can have three components depending on the lepton-pair angular momenta, $\Delta J_{\beta} = 0$, 1, and 2. The 1576 keV γ-transition has pure E2 character ($L_{\gamma} = 2$), and thus the A_{λ} parameters can be calculated without ambiguity.
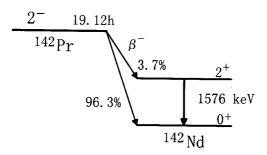
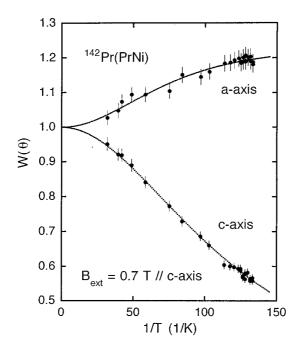**Fig. 1a.** Simplified decay scheme of ^{142}Pr.

Fig. 1b. Temperature dependence of 1576 keV γ anisotropy of ^{142}Pr in PrNi, measured at the a- and c-axes with an external field of $0\cdot7$ T along the c-axis.

The temperature dependence of the γ-anisotropy was measured at the a- and c-axes in an external field of $0\cdot7$ T along the c-axis. The function $W(\theta)$ in Fig. 1b is consistent with the magnetic structure of Pr ions. The observed γ anisotropy

is much larger than that previously seen (Grace *et al.* 1958; Daniels *et al.* 1958; Reid *et al.* 1969; Hirschfeld and Hoppes 1970; Smith and Weyhmann 1974). Indeed the magnitude of the anisotropy confirmed that the β decay proceeds mainly via the $\Delta J_\beta = 0$ nuclear matrix element, through the data analysis of the U_λ parameters (Nishimura *et al.* 1993).
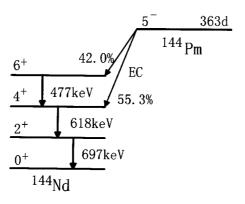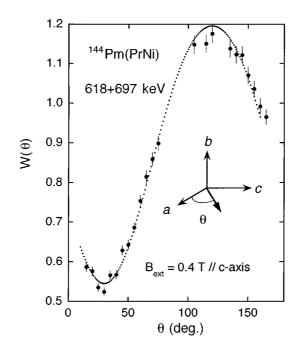
Fig. 2a. Simplified decay scheme of ^{144}Pm.

Fig. 2b. Angular distribution of averaged γ anisotropies of 618 and 696 keV transitions from oriented ^{144}Pm in PrNi in the b-plane. The external field of $0 \cdot 4$ T is along the c-axis. The angle is scaled from the a-axis.
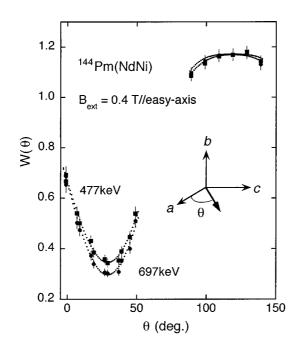
Fig. 2c. Angular distribution of γ anisotropies of 477 and 697 keV transitions from oriented ^{144}Pm in NdNi in the b-plane. The external field of $0\cdot4$ T is along the easy magnetisation direction: $24°$ from the a-axis in the b-plane.
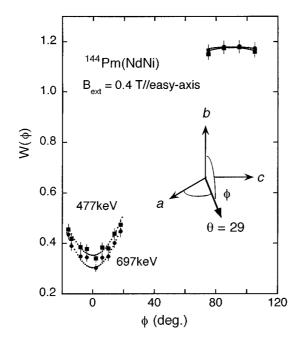

Fig. 2d. Angular distribution of γ anisotropy of ^{144}Pm in NdNi between the orientation axis and the b-axis. The angle ϕ is scaled from the orientation axis ($\theta = 29°$).

Using the U_λ parameters determined for the fit of the temperature dependence data, we extracted B_{HF} as 290(10) T, which is quite close to 272·2 T obtained from the spin-echo experiment of stable ^{141}Pr nuclei in $Pr_{0·2}Gd_{0·8}Ni$ (Shimizu *et al.* 1996). This work enables us to use ^{142}Pr as a probe nucleus in solid-state magnetism.

(3b) Magnetic Structure of Pm Ions in PrNi and NdNi

A simplified decay scheme of ^{144}Pm is shown in Fig. 2*a* (Firestone *et al.* 1996). The electron capture (EC) decay is first-forbidden $|\Delta I = 1|$, so that U_λ could have two terms corresponding to $\Delta J_\beta = 1$ and 2. The ratio $\delta^2 = U_\lambda(\Delta J_\beta = 2)/U_\lambda(\Delta J_\beta = 1)$ in the EC transition from the ground state $(I^\pi = 5^-)$ to the third excited state $(I^\pi = 6^+)$ has been determined from the course of present experiments as $\delta^2 = 0·0(+0·02)$, which means the β-decay matrix element of $\Delta J_\beta = 1$ is dominant (Nishimura *et al.* 1996).

Fig. 2*b* shows the γ angular distribution of ^{144}Pm in PrNi measured in the *b*-plane with an external field of 0·4 T along the *c*-axis (the easy-axis). The angle is scaled from the *a*-axis. It is obvious that the nuclear magnetic moments are oriented at an angle of about 30° with respect to the *a*-axis. HF produced by the 4f electrons of Pm ions are in the same direction. It is indeed surprising that the Pm ions of about 1 ppm form the different magnetic structure from that of the host PrNi.

NO of ^{144}Pm was also measured in the ferromagnetic compound of NdNi. The easy axis of NdNi is the *a*-axis at 28 K, and turns towards the *c*-axis in the *b*-plane below 15 K, subtending 24° from the *a*-axis (Fillion *et al.* 1984). Fig. 2*c* is the γ angular distribution of ^{144}Pm in NdNi in the *b*-plane. The minimum of $W(\theta)$ is in the 29(10)° direction from the *a*-axis. The γ angular distribution between the 29° direction and the *b*-axis is shown in Fig. 2*d*. The two figures clearly indicate that the Pm ions are ordered along the 29° direction, which is almost parallel to the easy-axis of NdNi. In NdNi, the Nd–Pm exchange interaction seems to be responsible for the observed magnetic structure of Pm ions.

The crystal electric field (CEF) effect is considered in order to understand the magnetic structures of the Pm ions. In CrB-type crystals, the *b*-axis is a special direction because the lattice constant of the *b*-axis is about twice as large as those of the *a*- and *c*-axes. There are many systems of the CrB-type compounds, in which this crystal asymmetry leads to the large magnetic anisotropy between the *b*-axis and the *b*-plane due to the CEF effect.

The known magnetic structures of PrNi, NdNi and SmNi are illustrated in Fig. 2*e*. SmNi has the same crystal structure as those of PrNi and NdNi, but the easy magnetisation direction is the *b*-axis (Isikawa *et al.* 1985). The easy magnetisation directions change from the *b*-plane to the *b*-axis between Nd and Sm ions. As described in the literature (Shohata 1977; Greedan and Rao 1973), such changes in magnetic structures have been attributed to the sign change in the second-order Stevens coefficient α_J between Nd^{3+} and Sm^{3+}. The α_J of Pr^{3+} and Nd^{3+} are positive values, but those of Sm^{3+} and Pm^{3+} are negative (Elliott and Stevens 1953). Therefore, as far as only the second-order CEF effect is concerned, Pm ions in PrNi and NdNi would order along the *b*-axis. The observed orientation axes of Pm ions seem to suggest that higher-order terms of CEF are important (Nishimura *et al.* 1996).
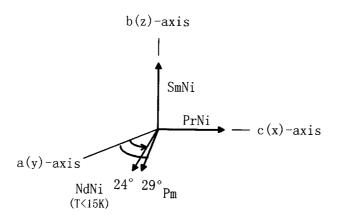
Fig. 2e. Magnetic structure of PrNi, NdNi and SmNi, and the observed orientation axis of ^{144}Pm nuclei in PrNi and NdNi. The electrical magnetic moments of NdNi order at 28 K along the a-axis, and below 15 K the moments order along the 24° direction from the a-axis in the b-plane.

The temperature dependence of the γ anisotropy is shown in Figs 2f and 2g. From the fit of those data to the $W(\theta)$ equation, we deduce that $B_{\mathrm{HF}}(\mathrm{PrNi}) = 185(48)$ T and $B_{\mathrm{HF}}(\mathrm{NdNi}) = 395(48)$ T. A theoretical value of B_{HF} for the Pm^{3+} free ion is 426 T (Bleaney 1972). The large reduction in $B_{\mathrm{HF}}(\mathrm{PrNi})$ suggests a possible understanding of the observed magnetic structures of the Pm ions. We believe that the magnetic structures of the Pm ions in PrNi and NdNi are the result of the balance of the CEF effect and the exchange interactions. Manufacture of a range of single crystals of $\mathrm{Pr}_x\mathrm{Nd}_{1-x}\mathrm{Ni}$ series will be undertaken in an attempt to understand the underlying mechanism leading to the magnetic structure of the Pm ions.

(3c) Non-axial Ordering of CeNi$_2$Al$_5$

CeNi$_2$Al$_5$ is a magnetic dense-Kondo compound with the Neel temperature of 2·6 K. The crystal structure is body-centred orthorhombic, which leads to a large magnetic anisotropy. The magnetic and thermal properties have been intensively studied (Isikawa *et al.* 1994). An NO experiment was carried out to obtain information on the magnetic structure of the ordered Ce ions using ^{141}Ce nuclei.

Fig. 3a shows the temperature dependence of the γ anisotropy measured along the three principal axes with an external field of 0·4 T along the b-axis. The γ anisotropy along the a-axis is represented by a single measurement at $1/T = 102$ K^{-1}. The important point is that the γ anisotropy along the a-axis appreciably deviates from that along the c-axis. This result tells us that the Ce ions have a non-axial magnetic structure.

When the nuclear ensemble lacks a single axis of orientation, the expression for $W(\theta)$ must be modified. If the full ensemble can be divided into two or more equivalent sub-ensembles, each of which has a simple axial symmetry, the combined angular distribution can be expressed as a sum of terms $W(\theta) = g_i W(\theta_i)$, with appropriate weights g_i for each term corresponding to the number of nuclei in
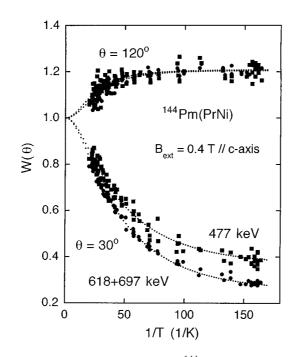
Fig. 2*f*. Temperature dependence of γ anisotropy of ^{144}Pm in PrNi. The detection directions are the orientation axis ($\theta = 30°$) and the perpendicular direction ($\theta = 120°$). The external field of $0 \cdot 4$ T is along the *c*-axis.
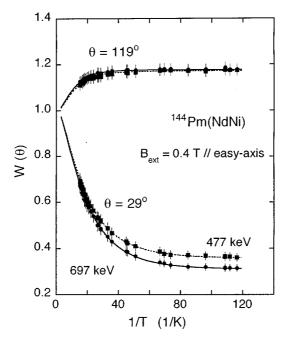

Fig. 2*g*. Temperature dependence of γ anisotropy of ^{144}Pm in NdNi. The detection directions are the orientation axis ($\theta = 29°$) and the perpendicular direction ($\theta = 119°$). The external field of $0 \cdot 4$ T is along the easy magnetisation axis (see Fig. 2*e*).
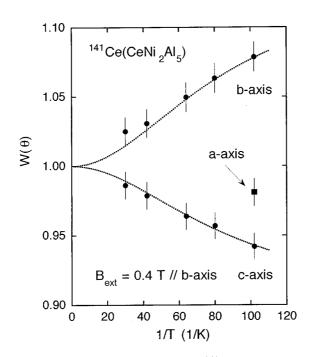
Fig. 3a. Temperature dependence of γ anisotropy of ^{141}Ce in CeNi$_2$Al$_5$ at the a-, b- and c-axes. The a-axis data are represented by a single square. The external field of $0\cdot 4$ T is along the b-axis.
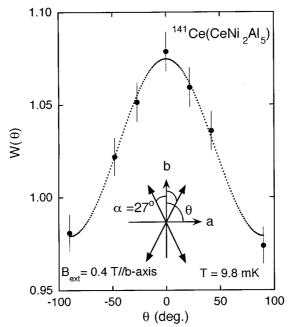

Fig. 3b. Angular distribution of γ anisotropy of ^{141}Ce in CeNi$_2$Al$_5$ in the c-plane. The angle is scaled from the b-axis. The line is the result of a fit to the magnetic structure indicated; antiferromagnetically ordered Ce moments are tilted by angles of $27°$ and $-27°$ from the b-axis.

that sub-ensemble (Turrell 1986). The data in Fig. 3a are not compatible with a simple uniaxial structure of the Ce electronic moments along the b-axis. Any such structure means that a- and c-axes are equivalent, both being at $\theta = 90°$ to the orientation axis.

We take the Ce moments as constrained to lie in the c-plane. Accordingly, we can fit the c-axis data to yield a B_{HF} of 92(6) T with the unique value of $\theta = 90°$. With this B_{HF} the angular distribution in the c-plane can be examined to give the magnetic structure of the Ce ions. Fig. 3b is the anisotropy as a function of angle θ measured from the b-axis in the c-plane at a base temperature of about $9·8$ mK; $\theta = 90°$ corresponds to the a-axis. The curve in Fig. 3b is the result of a fit assuming the two ensembles of Ce ions of aniferromagnetic structure, each subtending an angle of $27°$ from the b-axis. Neutron diffraction experiments gave a similar magnetic structure at $1·4$ K with an angle of $8°$ (Isikawa et $al.$ 1994). The magnetic structure of CeNi$_2$Al$_5$ is known to vary with temperature, so that the observed angle difference between the NO and neutron diffraction results may be attributed to the difference of base temperatures: $9·8$ mK for NO, $1·4$ K for neutron diffraction.

(3d) Co-existence of a Dense Kondo State with Magnetic Ordering

CeNi is an intermediate-valence compound, in which the cerium valence is said to vary from $3·5$ to $3·3$ between 4 and 300 K (Gignoux and Gomez-Sal 1985). Thermal expansion and magnetostriction studies support this character (Greuzet and Gignoux 1986). Applying pressure brought about a first-order transition observed in the resistivity and susceptibility (Gignoux and Voiron 1985). The de Hass–van Alphen effect experiments (Onuki et $al.$ 1989) and the band-energy calculation (Yamagami and Hasegawa 1991) offered evidence for an itinerant 4f-electron nature in CeNi.

There is a large number of studies substituting the Ce and/or Ni elements by other elements. In the CeNi$_x$Pt$_{1-x}$ series, the Ce ion state changes from the intermediate-valence state to a ferromagnetic state in the range $x < 0·9$ (Gignoux and Gomez-Sal 1984). It is a matter of the position of the 4f level relative to the Fermi level; the 4f level is deep below the Fermi level in CePt, and is very close to it in CeNi. The Kondo impurity state appears in the series of Ce$_x$La$_{1-x}$Ni ($x < 0·7$) (Isikawa et $al.$ 1986). These variations suggest a general rule: The 4f level and conduction-band hybridisation increases as the cell volume decreases.

In this view, the RKKY exchange interactions are treated as a competing effect with the Kondo effect. It is generally agreed that a single ground state is formed when the Kondo effect is stronger than the RKKY interactions which favour magnetic ordering (Yamamoto and Ohkawa 1988). Our problem is to determine the nature of a Ce ion site when it is surrounded by magnetic ions, or of a magnetic ion site surrounded by Ce ions.

NO of the Ce$_x$Nd$_{1-x}$Ni series has been done for $x = 0·0$, $0·1$, $0·25$, $0·5$ and $0·8$, using the γ transitions of 145 keV from ^{141}Ce and 531 keV from ^{147}Nd. The results show that the compounds magnetically order due to Nd–Nd exchange interactions over the whole range of x studied, and no magnetic ordering occurs on the Ce ions (Oliveira et $al.$ 1994). From the temperature dependence of the γ anisotropy of ^{147}Nd, the extracted B_{HF} are plotted in Fig. 4a as ratios for each concentration $(1-x)$ to B_{HF} of NdNi (418 T). Ratios of the magnetisation along
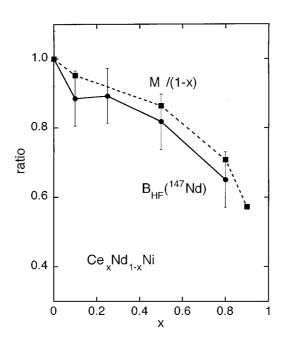
Fig. 4a. Comparison between normalised hyperfine fields in Nd nuclear sites and normalised magnetic moments of Nd ions in $Ce_xNd_{1-x}Ni$; for $x = 0$, $B_{HF} = 418$ T and $M = 2 \cdot 50 \, \mu_B$.

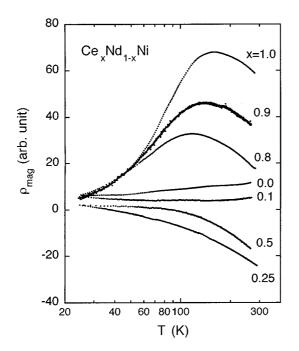**Fig. 4b.** Magnetic part of resistivity of $Ce_xNd_{1-x}Ni$ versus $\ln(T)$, where $\rho_m = \rho(T) - \rho_0(T=4 \cdot 2 \text{ K}) - \rho_p(\text{LaNi})$.

the a-axis, normalised by $(1-x)$ at an external field of 0.7 T to that of NdNi ($2.5\,\mu_{\mathrm{B}}$), are also shown in the figure. It is noted that these ratios similarly decrease as the Nd concentrations $(1-x)$ decrease.

The Kondo effect exists on the Ce ion sites. Fig. $4b$ shows the magnetic part of the resistivity ρ_{m}, which was estimated by subtracting the residual resistivity ρ_0 at 4.2 K and the resistivity of LaNi ρ_{p} as a phonon contribution from the measured resistivity ρ; i.e. $\rho_{\mathrm{m}} = \rho - \rho_0 - \rho_{\mathrm{p}}$. The $-\ln T$ dependence of ρ_{m} due to the Kondo effect is noticeable. Further evidence for the Kondo effect in the series can be seen in the thermopower. Fig. $4c$ shows the results of thermopower measurements with a temperature gradient along the a-axis. The sensitivity of the thermopower to the Kondo effect is clear if one compares the magnetic resistivity and the thermopower for $x = 0.0$ and 0.1. Large values of the thermopower have been quite often observed in Kondo compounds, and have been ascribed to the formation of a narrow peak in the electron state density near the Fermi level due to the correlation between the 4f electrons of Ce ions and the conduction electrons (Sakurai *et al.* 1987).
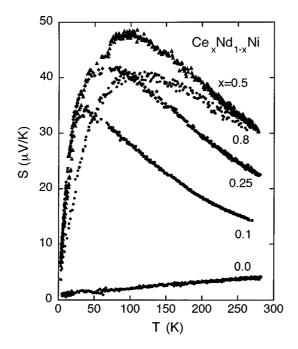

Fig. 4c. Thermoelectric power of $Ce_x Nd_{1-x} Ni$ versus T, where a temperature gradient is along the a-axis.

The most striking aspect of NO results is that the magnetic ordering of Nd ion sites was observed as being independent of the magnetism of the Ce ions. The magnetic properties of the whole $Ce_x Nd_{1-x} Ni$ series were found to remain remarkably like NdNi, even for $x = 0.8$ where on average each Nd ion is surrounded by Ce ions. This latter result prompted us to look in more detail at the magnetic properties for $x = 0.8$.
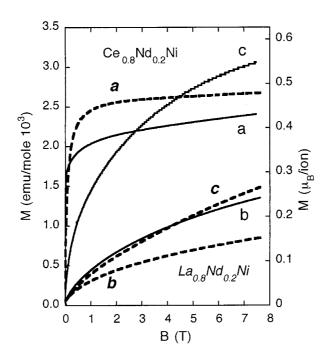
Fig. 5a. Magnetisation of $Ce_{0.8}Nd_{0.2}Ni$ (solid curves) and $La_{0.8}Nd_{0.2}Ni$ (broken curves) at 2 K along the a-, b- and c-axes.

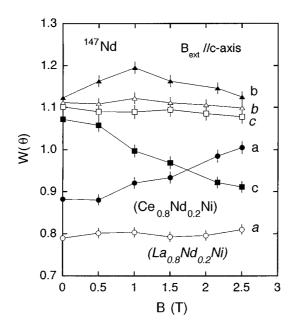**Fig. 5b.** Field dependence of γ anisotropy of ^{147}Nd in $Ce_{0.8}Nd_{0.2}Ni$ (open symbols) and $La_{0.8}Nd_{0.2}Ni$ (closed symbols) at the a-axis (circles), b-axis (triangles) and c-axis (squares). The external field is applied along the c-axis.

(3e) Magnetic Properties of $Ce_{0.8}Nd_{0.2}Ni$ and $La_{0.8}Nd_{0.2}Ni$

From NO experiments on the $Ce_xNd_{1-x}Ni$ series, we have the impression that the Ce–Nd interactions are quite weak. The competition between the RKKY and Kondo states is unknown. One important factor in this competition is whether the 4f electrons from the Ce ions in a delocalised state participate in the exchange interaction between the Nd ions. In an attempt to answer this question we made a single crystal of $La_{0.8}Nd_{0.2}Ni$.

The magnetisation M of $Ce_{0.8}Nd_{0.2}Ni$ and $La_{0.8}Nd_{0.2}Ni$ was measured along the a-, b- and c-axes at 2 K, as shown in Fig. 5a. $La_{0.8}Nd_{0.2}Ni$ has a large magnetic anisotropy between the a-axis and the a-plane. The M value for $Ce_{0.8}Nd_{0.2}Ni$ along the c-axis exceeds, peculiarly, that along the a-axis. Initially from these data we wrongly imagined that the Ce ions made a large contribution to M along the c-axis because CeNi is known to behave as an enhanced Pauli paramagnet with an external field along the c-axis (Fillion *et al.* 1984).

NO is sensitive to changes in the direction of the HF, which is parallel to the bulk M. Thus, changes in the direction of M will result in changes in the γ anisotropy. Fig. 5b shows the dependence of the γ anisotropy of ^{147}Nd in $Ce_{0.8}Nd_{0.2}Ni$ and $La_{0.8}Nd_{0.2}Ni$, detected at the a-, b- and c-axes, as a function of an external field, kept along the c-axis. The $W(a)$ and $W(c)$ change in magnitude in $Ce_{0.8}Nd_{0.2}Ni$, but change little in $La_{0.8}Nd_{0.2}Ni$. The data show the nuclear spin re-orientation of ^{147}Nd in $Ce_{0.8}Nd_{0.2}Ni$, which is equivalent to the re-arrangement of the electronic moments of Nd ions.

The extra component of M for $Ce_{0.8}Nd_{0.2}Ni$ along the c-axis compared to that along the a-axis, therefore, originates in M of the Nd ions, and is attributed

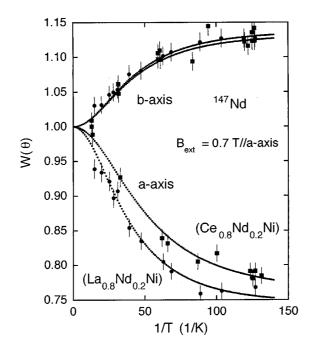**Fig. 5c.** Temperature dependence of γ anisotropy of ^{147}Nd in $Ce_{0.8}Nd_{0.2}Ni$ (squares) and $La_{0.8}Nd_{0.2}Ni$ (circles) at the a- and b-axes. The external field of 0·7 T is along the a-axis.

to the re-arrangement of the Nd electronic moments. In short, the electronic structure of the Nd ions in $Ce_{0.8}Nd_{0.2}Ni$ is different from that in $La_{0.8}Nd_{0.2}Ni$. The temperature dependence of the γ anisotropy of ^{147}Nd in $Ce_{0.8}Nd_{0.2}Ni$ and $La_{0.8}Nd_{0.2}Ni$, shown in Fig. 5c, yields a B_{HF} of 272(18) T and 340 (10) T respectively (Doran *et al.* 1995). Although B_{HF} in $Ce_{0.8}Nd_{0.2}Ni$ is smaller than that in $La_{0.8}Nd_{0.2}Ni$, this difference could not be attributed only to the Ce–Nd interactions. It is possibly caused by the different electronic structure of the Nd ions in those compounds.

Without NO results we would continue to have the wrong impression that the Ce ions produced large contributions to M along the c-axis. Since in NO experiments a geometrical arrangement of detectors is independent of the external field direction, this kind of measurement can be done easily. The interactions between the Ce and Nd ions in the series, however, remain unknown. We have a plan to perform NO on the $Ce_xGd_{1-x}Ni$ series to elucidate the competition between the RKKY and Kondo states.

(3f) Nuclear Parameters and Hyperfine Field

We list the extracted and adopted nuclear decay parameters, as well as the B_{HF} values experienced by relevant isotopes studied:

$$^{141}Ce: \quad 145 \text{ keV}, \quad U_2 A_2 = 0.1583^A,$$

$$U_4 A_4 = 0.0017^A, \quad B_{HF}(CeNi_2Al_5) = 92(6) \text{ T};$$

$$^{142}Pr: \quad 1576 \text{ keV}, \ U_2 A_2 = -0.562,$$

$$U_4 A_4 = -0.854, \quad B_{HF}(PrNi) = 290(10) \text{ T};$$

$$^{147}Nd: \quad 531 \text{ keV}, \quad U_2 A_2 = -0.209^B,$$

$$U_4 A_4 = -0.02^B, \quad B_{HF}(NdNi) = 418(12)T;$$

$$^{144}Pm: \quad 477 \text{ keV}, \quad U_2 A_2 = -0.3860,$$

$$U_4 A_4 = -0.1796, \quad B_{HF}(PrNi) = 185(48) \text{ T};$$

$$^{144}Pm: \quad 477 \text{ keV}, \quad B_{HF}(NdNi) = 395(48) \text{ T};$$

where the superscripts A and B refer to Rijswijk *et al.* (1982) and Al-Janabi *et al.* (1977) respectively.

4. Future Applications

NMR on oriented nuclei (NMRON) is an advanced technique combining NMR precision and NO sensitivity (Stone 1986). This technique has been widely used mainly in nuclear physics to measure electromagnetic moments of radioactive nuclei. Usually, probe nuclei are doped into soft magnetic materials such as Fe, Co and Ni. Compared with conventional NMR, NMRON is free from the domain-wall problem because almost all probe nuclei are in domains.

The pulsed-NMRON developed in Canberra (Chaplin and Wilson 1986) is quite attractive to study rare earth intermetallics because large pulsed rf-fields can overcome the magnetic anisotropy originating in 4f electron orbital motions. In the present study of $Ce_xNd_{1-x}Ni$, we have obtained the averaged B_{HF} experienced by ^{147}Nd nuclei. Pulsed-NMRON of ^{147}Nd in this system will provide a precise distribution of B_{HF} and a HF direction, which could enable us to estimate the Ce–Nd interaction strength.

Quite recently, we were informed that the Canberra NO group has succeeded in the thermometric detection of NMR of a Yb compound. This is a novel method for observing a resonance of a stable isotope: (1) a sample contains probe radioactive nuclei which work as a nuclear thermometer; (2) a base temperature is low enough to achieve the nuclear orientation of the probe nuclei; (3) an rf frequency is set to a resonance frequency of stable nuclei under study; (4) when the stable nuclei resonate, the sample absorbs the rf power resulting in warming the sample; and (5) the change in the temperature is detected by the nuclear thermometer.

The first successful thermometric detection was made in $MnCl_2 \cdot 4H_2O$ (Kotlicki and Turrell 1986). In Co metals, the frequency shift due to the nuclear spin magnetism was observed (Seewald *et al*. 1996). We are interested in the thermometric detection of NMR in NdNi compounds. We have observed the magnetic hyperfine-interaction frequency of ^{143}Nd in NdNi at about 822 MHz, and the data for ^{147}Nd nuclear thermometry have also been accumulated.

Acknowledgments

References

Al-Janabi, T., Hamilton, W. D., and Warner, D. D. (1977). *J. Phys.* G **3**, 1415.
Bleaney, B. (1972). *In* 'Magnetic Properties of Rare Earth Metals' (Ed. R. J. Elliott), Ch. 8 (Plenum: New York).
Chaplin, D. H., and Wilson, G. V. H. (1986). *In* 'Low-Temperature Nuclear Orientation' (Eds N. J. Stone and H. Postma), Ch. 14 (North Holland: Amsterdam).
Daniels, J. M., LaMarche, J. L. G., and LeBlanc, M. A. R. (1958). *Can. J. Phys.* **36**, 997.
Doran, D., Isikawa, Y., Nishimura, K., Oliveira, I. S., Stone, N. J., Veskovic, M., Williams, D. A. (1996). *Hyp. Interact.* C **1**, 139.
Elliott, R. J., and Stevens, K. W. H. (1953). *Proc. R. Soc. London* A **218**, 553.
Fillion, G., Gignoux, D., Givord, F., and Lemaire, R. (1984). *J. Mag. Magn. Mater.* **44**, 173.
Firestone, R. B., Shirley, V. S., Baglin, C. M., Frank Chu, S. Y., and Zipkin, J. (1996). *In* 'Table of Isotopes', 8th edn (Wiley: New York).
Gignoux, D., and Gomez-Sal, J. C. (1984). *Phys. Rev.* B **30**, 3967.
Gignoux, D., and Gomez-Sal, J. C. (1985). *J. Appl. Phys.* **57**, 3125.
Gignoux, D., and Voiron, J. (1985). *Phys. Rev.* B **32**, 4822.
Grace, M. A., Johnson, C. E., Scurlock, R. G., and Taylor, R. T. (1958). *Phil. Mag.* **3**, 456.
Greedan, J. E., and Rao, V. U. S. (1973). *J. Solid State Chem.* **6**, 387.
Greuzet, G., and Gignoux, D. (1986). *Phys. Rev.* B **33**, 515.

Hirschfeld, A. T., and Hoppes, D. D. (1970). *Bull. Am. Phys. Soc.* **15**, 628.

Isikawa, Y., Mori, K., Ueno, K., Sato, K., and Maezawa, K. (1985). *J. Mag. Magn. Mater.* **52**, 434.

Isikawa, Y., Mori, K., Fujii, A., and Sato, K. (1986). *J. Phys. Soc. Jpn* **55**, 3165.

Isikawa, K., Mizushima, T., Sakurai, J., Mori, K., Munoz, A., Givord, F., Boucherle, J. X., Voiron, J., Oliveira, I. S., and Flouquet, J. (1994). *J. Phys. Soc. Jpn* **63,** 2349.

Kotlicki, A., and Turrell, B. G. (1986). *Phys. Rev. Lett.* **56**, 773.

Krane, K. S. (1986). *In* 'Low-Temperature Nuclear Orientation' (Eds N. J. Stone and H. Postma), Ch. 2 (North Holland: Amsterdam).

Nishimura, K., Oliveira, I. S., Stone, N. J., Isikawa, Y., Shimizu, K., and Sato, K. (1993). *Hyp. Interact.* **78**, 153.

Nishimura, K., Mori, K., Ohya, S., Muto, S., and Isikawa, Y. (1996). *Phys. Rev.* B **53**, 15010.

Oliveira, I. S., Nishimura, K., Stone, N. J., Isikawa, Y., Zakoucky, D., and Doran, D. (1994). *Phys. Rev.* B **49**, 11886.

Onuki, Y., Kurosawa, Y., Maezawa, K., Zuru, I., Isikawa, Y., and Sato, K. (1989). *J. Phys. Soc. Jpn* **58**, 3705.

Reid, P. G. E., Stone, N. J., Bernas, H., Spanjaard, D., and Campbell, I. A. (1969). *Proc. R. Soc. London* A **311**, 169.

Rijswijk, W. van, Berg, F. G. van den, Keus, H. E., and Huiskamp, W. J. (1982). *Physica* B **113**, 127.

Sakurai, J., Ohyama, T., and Komura, Y. (1987). *J. Mag. Magn. Mater.* **63&64**, 578.

Seewald, G., Hagn, E., and Zech, E. (1996). Proc. 10th Int. Conf. on Hyperfine Interactions, Part 2, p. 29 (Leuven: Belgium).

Shimizu, K., Ichinose, K., and Nishimura, K. (1996). *J. Phys. Soc. Jpn* **65**, 2736.

Shohata, N. (1977). *J. Phys. Soc. Jpn* **42**, 1873.

Smith, C. H., and Weyhmann, W. V. (1974). *Phys. Lett.* B **52**, 195.

Stone, N. J. (1986). *In* 'Low-Temperature Nuclear Orientation' (Eds N. J. Stone and H. Postma), Ch. 13 (North Holland: Amsterdam).

Stone, N. J., and Postma, H. (Eds) (1986). *In* 'Low-Temperature Nuclear Orientation', Ch. 1 (North Holland: Amsterdam).

Turrell, B. G. (1986). *In* 'Low-Temperature Nuclear Orientation' (Eds N. J. Stone and H. Postma), Ch. 10 (North Holland: Amsterdam).

Yamagami, H., and Hasegawa, A. (1991). *J. Phys. Soc. Jpn* **60**, 1011.

Yamamoto, T., and Ohkawa, F. J. (1988). *J. Phys. Soc. Jpn* **57**, 3562.